Impact of air infiltration rates on moisture buffering effect of wooden surfaces

Dimitrios Kraniotis[*1], Tormod Aurlien[2], Christoph Brückner[1] and Kristine Nore[1]

1 Norwegian Institute of Wood Technology
Forskningsveien 3B
0373 Oslo, Norway

2 Norwegian University of Life Sciences
Drøbakveien 31, P.O. box: 5003 IMT,
1432 Ås, Norway

**Corresponding author: dimitrios.kraniotis@treteknisk.no*

ABSTRACT

Interior wooden surfaces have the capacity to buffer the maxima and minima of relative humidity (RH) indoors. Especially in high performance buildings, where high airtightness levels as well as high indoor air quality (IAQ) are required, there is great potential for energy savings by reducing the mechanical ventilation demand. The last decade, the moisture buffer phenomena has been widely researched. Relevant findings showed that the moisture buffering effect is reduced when the ventilation rates increase. The air infiltration is usually taken into consideration simply as an additional fraction of air exchange. However, infiltration has a rather complex nature and can result into more localized effects compared to ventilation (mechanical) that mostly applies globally to a room. In this paper, the moisture buffering phenomena linked to the variation of air infiltration rates are studied in a cross laminated timber (CLT) test house. Both CO_2 and moisture are released in the room. The infiltration rates are calculated using tracer gas techniques (CO_2 decay method), while the air exchanges are calculated based on the decay of RH as well and the results are compared. In addition, the indoor relative humidity (RH) and moisture content in the construction elements are measured in different monitoring positions. The impact of airtightness and infiltration rates on the overall ('global') moisture buffer capacity is studied. Furthermore, the influence of the leakage location on the 'local' moisture buffer capacity of each monitoring position / element is also tested. Finally, the potential of using moisture is as 'tracer gas' for estimating the air exchanges in a room is researched.

KEYWORDS

moisture buffering, air infiltration, tracer gas techniques, air exchanges, moisture content

1 INTRODUCTION

The last decade the awareness of influence of hygroscopic materials use in buildings has increased. The moisture buffer capacity has been analysed in several studies (e.g. Simonson *et al.*, 2001; Rode *et al.*, 2005; Osanyintola *et al.*, 2006). The results show that hygroscopic materials hold a great potential to damp the maxima and minima of relative humidity (RH), narrowing the range of the latter. This fact results in reduction of ventilation loads and

consequently on the energy savings. In addition, it secures a better indoor microclimate, which is not too humid nor too dry. In particular, Simonson *et al.* (Simonson *et al.*, 2001) showed that when the internal surfaces of a wooden apartment building were permeable, the maximum indoor RH was lower compared to the impermeable case assumed (impermeable paint). In addition, the RH dropped below 20% for less period of time compared to the impermeable case.

The potential indirect savings from adjusting the ventilation rate and indoor temperature while maintaining adequate indoor air quality and comfort are in the order of 5 % for heating while they range from 5% to 20% for cooling. Woloszyn *et al.* (Woloszyn *et al.*, 2009) confirmed that the use of gypsum-based moisture-buffering materials is an efficient way combined with a relative humidity sensitive (RHS) ventilation system could reduce the mean ventilation rate of 30% – 40% and generate 12% – 17% of energy savings in the cold period. It was even possible, by the combined effect of ventilation and wood as buffering material to keep the indoor RH at a stable level, between 43% and 59%.

One of the 'non-material' parameters that affect the moisture buffer capacity of surfaces is ventilation by means of both mechanical and natural (Simonson *et al.*, 2004). Higher ventilation rates result in reduced buffering effect (Yoshino *et al.*, 2009). Usually, the infiltration is taken into account only as a constant fraction of the total air exchanges (Rode *et al.*, 2008) or it is even neglected for simplification reasons (Yang *et al.*, 2014). Yang *et al.* (Yang *et al.*, 2012) and Li *et al.* (Li. *et al.*, 2012) have included infiltration in their models when evaluating moisture buffer capacity of wooden interior surfaces in an environmental chamber. Moreover, the dynamic nature of air infiltration have been recognized (Haghighat *et al.*, 2000). Taking into account the natural unsteady characteristics of air infiltration and their impact on estimating better the air exchanges has been presented (Kraniotis *et al.*, 2014).

This study explores the impact of in-situ-measured infiltration rates on the moisture buffer capacity (drying process) of hygroscopic surfaces. The experiment has been conducted in a cross-laminated-timber (CLT) test house with controlled leakages. A previous study conducted in the same test house showed how the mechanical ventilation rates affect the levels of indoors RH and the moisture buffering in the wooden structure (Katavic *et al.*, 2014). In the current paper, the focus is on the influence of air infiltration on the moisture buffer capacity, and thus the mechanical ventilation is shut down. The study compares the 'global' (overall) infiltration rate with the corresponding decay of the indoor RH. Carbon dioxide (CO_2) is used as tracer gas and the concentration decay method for calculating the infiltration rates (exfiltration). Furthermore, localizing the leakages allows the deeper investigation of the influence of air infiltration on the moisture buffer capacity of the wooden surfaces. The air exchanges of the test house are estimated using both traditional tracer gas techniques (CO_2) as well as the decay of the RH levels indoors. Thus, an evaluation of the potential of using moisture as 'tracer gas' is presented.

2 METHODOLOGY

2.1 Experimental site

The experimental facilities consists of a test house located in a meteorological field, affiliated to the Norwegian University of Life Sciences (NMBU), Ås, Norway. The single-compartment test house is constructed of CLT made of spruce and is insulated with mineral wool. The thickness of the walls is 100mm, while the ceiling is 140mm thick. The test house is externally insulated; 100mm mineral wool in the South and East wall, 150mm in the North and West and 250mm in the roof. Two layers of open-diffusive weather resistant barriers (wind barriers) have been placed; one on the interior side of the insulation layer and one on

the exterior side. The roof has only the internal layer of wind barrier. Fig. 1 shows a cross section of the South wall of the test module.
The floor has 14 mm oak parquet over 22 mm chipboard and 100 mm mineral wool insulation. The modules are placed on top of 200 mm Rockwool with vapour barrier inhibiting any moisture to penetrate from the ground. The internal dimensions of the modules are 7.0m x 3.6m, while the net height of the room is 2.24m (Fig. 2a, 2b).

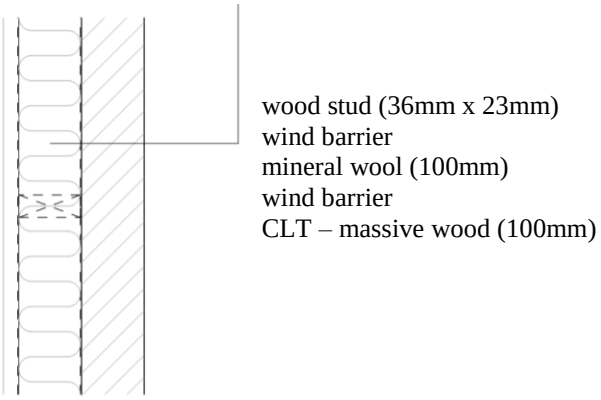

Figure 1: Cross section of the external wall (South) of the test house.

The leakage area of the room consists of 8 holes, of circular section of diameter δ = 16mm (A $\approx$ 2cm^2), that cross the whole assembly of the South and the North walls. They are located as 'pairs' in four positions of the walls. The leakages are noted as e_1 – e_8 and are shown in Fig. 2a and 2b. The lower ones, i.e. e_1, e_3, e_5 and e_7, are 120mm above the floor, while the upper ones, i.e. e_2, e_4, e_6 and e_8, are 270mm above the floor (Fig. 3a).

2.2 Structure of experiment

The experiment consisted of 3 phases:

- Phase 1: the moisture release (moisture generation) and mixing – wetting phase,
- Phase 2: the CO_2 release and mixing and
- Phase 3: the 'decay' phase – drying.

The moisture release lasted for 8 hours and a humidifier, in the centre of the room (noted by b in Fig. 2a, 2b), was used for the moisture generation in a constant rate (375g/h). In order to ensure sufficient moisture mixing and thus uniformity within the room, two fans were used located diametrically at the NE and the SW corner of the test house, noted as c_1 and c_2 in Fig. 2a and 2b. During this phase the leakages were hermetically sealed, thus it is assumed that the released moisture migrates and is getting absorbed by the hygroscopic CLT panels.
After 8 hours, the humidifier was turned off and the CO_2 was released. The fans were working for 10min more in order to ensure the sufficient mixing of the gas and guarantee that the required uniformity (ASTM – E741-06, 2006).
The previous short phase follows the 'decay phase' and the drying out of the wooden structure. The CO_2 concentration decay method was used to calculate the infiltration rates. In order to ensure reliability of the rates, the duration of this last phase was determined as 24h, respecting the requirements of the relevant standards.
In total, the experiment consists of six measurements. Three experiments were conducted will all the eight holes open during the phase 3 (decay – drying) and they are noted as A_1 – A_3. In addition, three measurements were executed with only the four holes open, i.e. e_1, e_2, e_7 and e_8, means the holes located at the 'east' part of the room. The rest of the holes remained sealed, i.e. e_3, e_4, e_5 and e_6. These three measurements are noted as A_4 – A_6.

2.3 Instrumentation

The CO_2 concentration was measured and recorded using CO_2 loggers that had been placed in five positions, i.e. d_1 – d_5 in Fig. 2a and 2b. The loggers have also the possibility to measure and log temperature T and relative humidity RH. The current set-up aims: i) to confirm the sufficient spatial distribution of CO_2 and moisture by monitoring the [CO_2] and the indoors RH in five different positions (phase 1 and 2) and ii) to detect possible differences during the last phase 3, as the loggers had been strategically placed, i.e. d_1 at the centre of the room, d_2 - d_3 close to the leakages at the 'west' part of the room and d_4 - d_5 close to the ones at the 'east' part. In addition, the loggers d_2 and d_4 have been placed on a lower height, i.e. 550mm, while the d_3 and d_5 in a higher height, i.e. 1940mm. The logger d_1 is on level 900mm above the floor at the centre of the room (Fig. 2b).

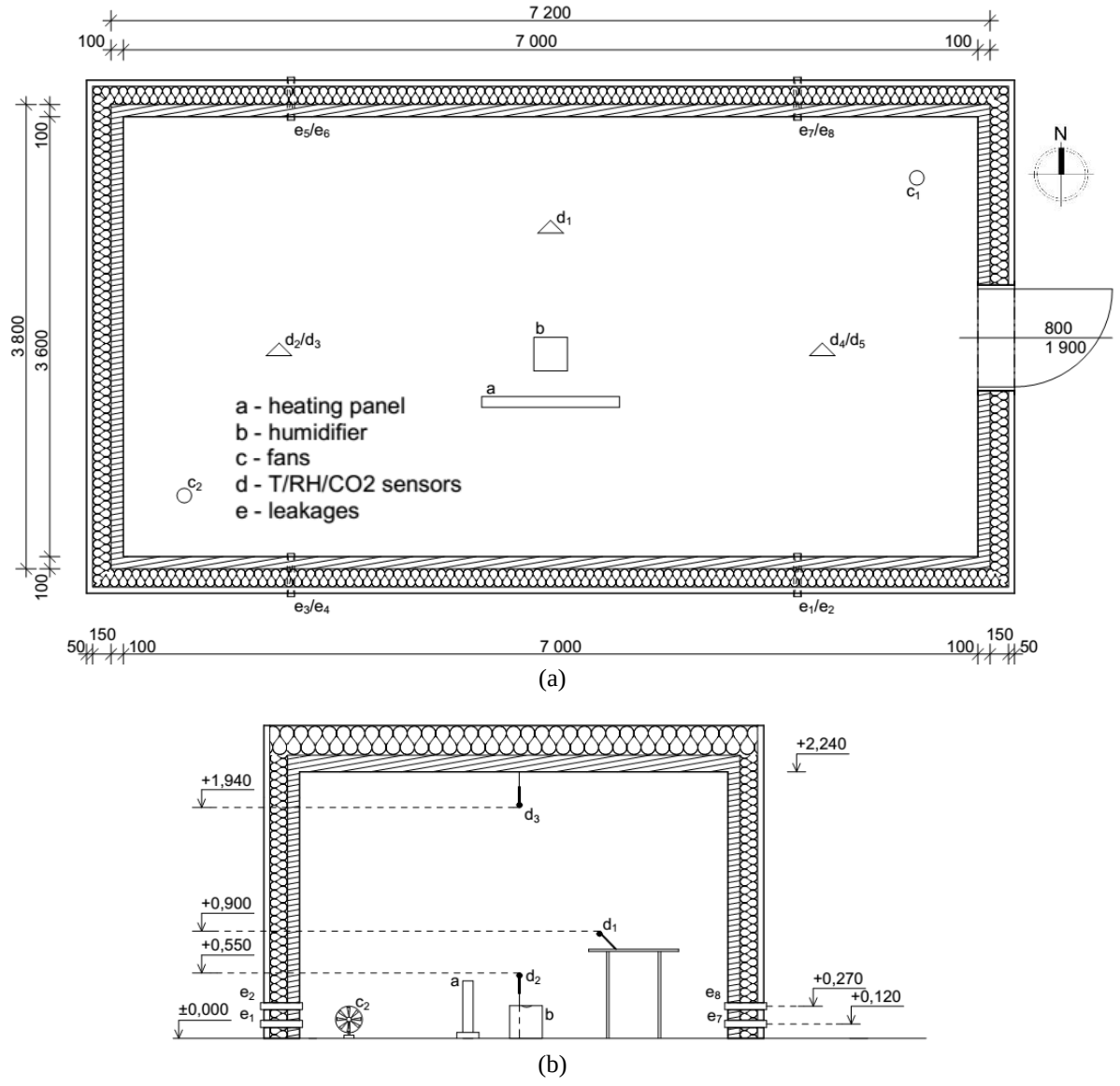

Figure 2: (a) Plan view and (b) cross section of the test house, where schematic representation and positions of the instruments used are shown.

In addition, 15 sensors that measure the equilibrium moisture content (EMC) in the CLT panels have been mounted in characteristic positions, i.e. 'aligned' with cross sections of the leakages and at a lower and medium height (750mm and 1500mm respectively). The sensors also record also T and RH locally. They are noted by 'H_1-H_{15}' and the exact positions are shown in Fig. 3.

Finally, the test house is equipped with an electric heating system to maintain the indoor temperature at 20°C. Technically an extract ventilation system exists, but the since the objective of the study was to investigate the phenomena linked to infiltration, the ventilation was shut down and the exhaust was sealed throughout the experiment.

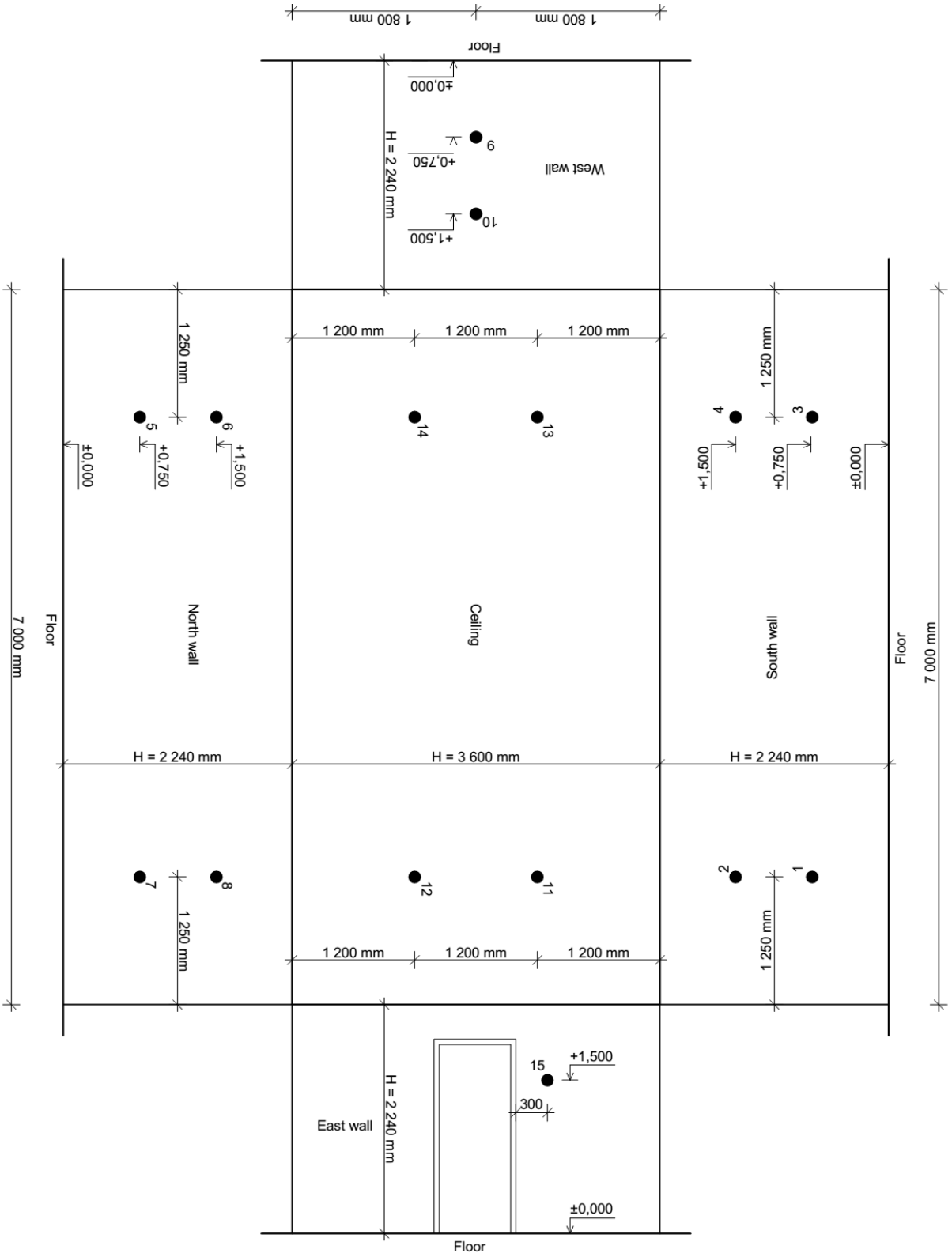

Figure 3: Plan view of the ceiling and view of the four walls that show the positions of the T/RH/EMC sensors.

2.4 Calculation of infiltration rates (decay of [CO_2])

The infiltration rates were calculated based on the relevant methodology described in the standard ASTM – E741-06 regarding the 'concentration test decay method' (ASTM – E741-06, 2006). For each day, the initial and final times are determined and a normalized concentration C_N is calculated in each measurement (Roulet *et al.*, 2002):

$$C_N = \frac{C(t) - C_o}{C(0) - C_o} \quad (1)$$

where C(t) the average CO_2 concentration in the test room, C(0) the initial CO_2 concentration in the test room, C_o the outdoors CO_2 concentration (≈ 400ppm) and t the time.
Since the CO_2 concentration fluctuating as decaying the 'average method' cannot be applied. Thus, in order to compute the ACH, the 'optional regression method' is used and a regression of ln*C(t)* needs to be performed according to (ASTM – E741, 2006):

$$ln\, C_N = -At + ln\, C_N\,(0) \quad (2)$$

The infiltration rates are represented by the fit line calculated after the regression analysis and in particular by the slope of the lnC_N against the time.

2.5 Decay of indoor RH

The decrease of the RH was also recorded simultaneously with the decay of the CO_2 concentration. During the last phase 3, the decline of the moisture content in the room is caused by the air leakages. To calculate the air exchanges using the reading of humidity, the vapor concentrations indoors and outdoors are needed. The volumetric concentration is given as:

$$Cv = \frac{p_w}{P} \quad (3)$$

where C_v is the concentration of water in air (as a ratio of water vapor volume to total wet air volume), p_w the partial water vapor pressure and P the total system pressure.
The RH is defined as the ratio of water vapor pressure p_w to the saturation water vapor pressure (p_{ws}) at the gas temperature:

$$RH = \frac{p_w}{p_{ws(T)}} 100\% \quad (4)$$

$$p_w = RH * p_{ws(T)} * 100\% \quad (5)$$

The $p_{ws(T)}$ is calculated as follows:

$$p_{ws(T)} = e^{(77.3450 + 0.0057T - \frac{7235}{T})} / T^{8.2} \quad (6)$$

Assuming the atmospheric pressure as the total system pressure P, the C_v calculation is feasible for both indoors and outdoors, i.e. $C_v(t)$ and C_{vo}, using the T and the RH inside the room and the ambient air respectively. A normalized concentration C_{vN} is calculated for each measurement:

$$C_{vN} = \frac{C_v(t) - C_{vo}}{C_v(0) - C_{vo}} \quad (7)$$

In analogous way to the previous infiltration rate (CO_2 decay), the current 'moisture-based' infiltration rate is a natural logarithm function over time. The slope of the function in a semi-log graph gives the infiltration rate.

3 RESULTS

The whole measurement period for the day A_5 is presented as example in Fig. 4. The wetting phase (phase 1) is clear, which lasted for 8h, as well as the phase of decay (phase 3). The RH increased during moistening of the room, while the concentration of CO_2 stayed stable, just somewhat higher than the outdoors levels. After the phase 1, the humidifier was turned off and the release/mixing of CO_2 started (phase 2). Right after only 10min, the phase 3 started.

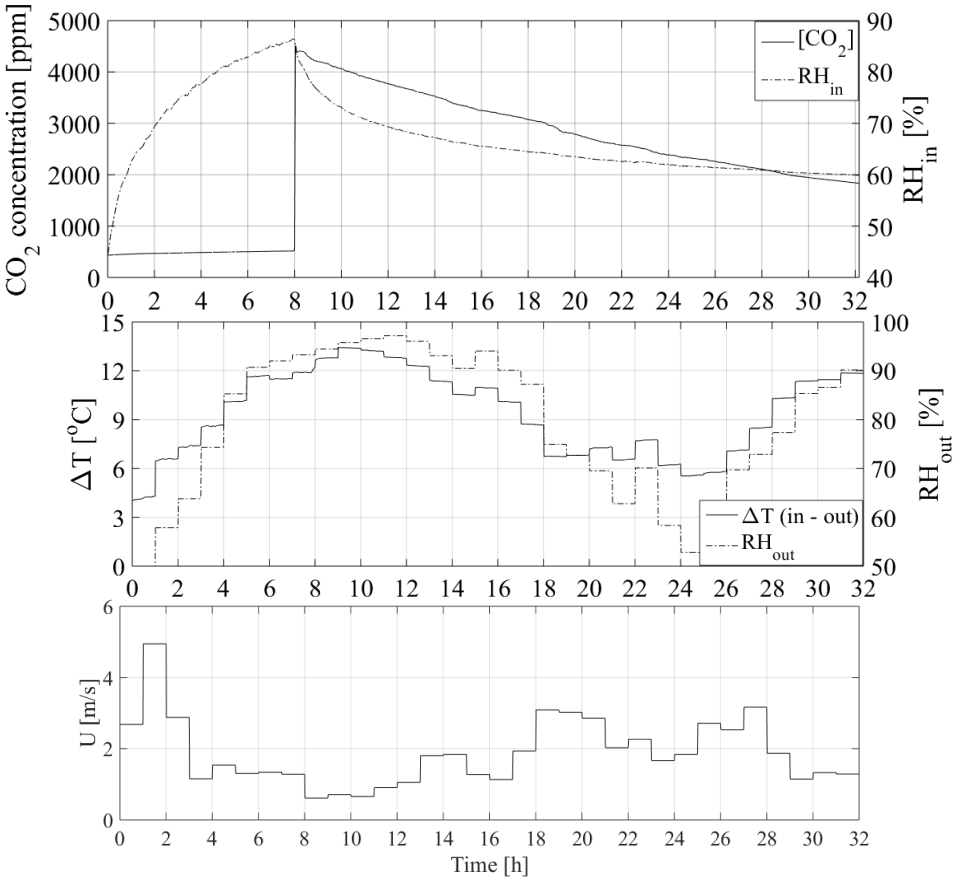

Figure 4: Overview of whole measurement period for test A_5. The variation of $[CO_2]$ and RH_{in} is shown as well as the time series of RH_{out}, temperature difference ΔT and wind speed U.

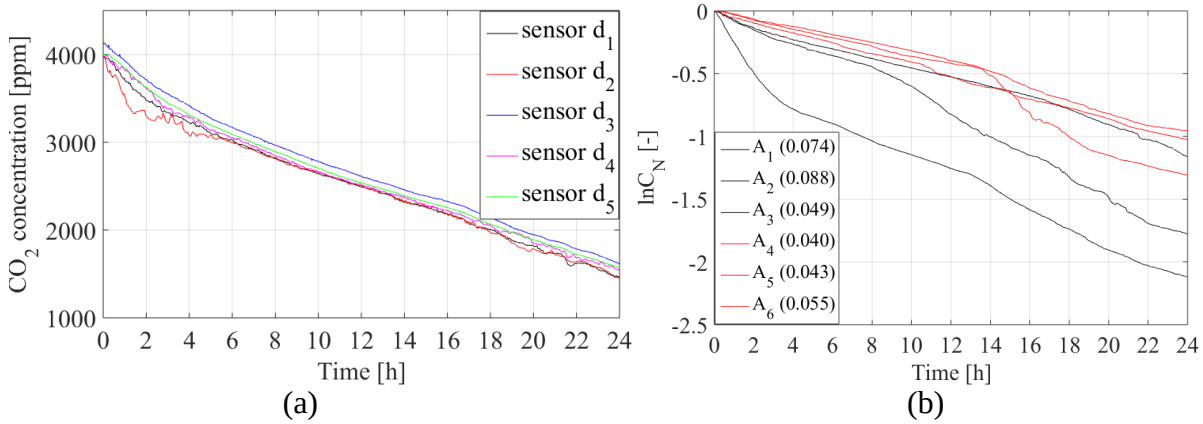

Figure 5: (a) The decay of $[CO_2]$ as recorded at the five positions (d_1 – d_5) during the test A_3. (b) The infiltration rates (averaged positions) calculated for the six measurements (A_1 – A_6).

Table 1: Infiltration rates based on the CO2 decay and the decay of the indoors RH.

Measurement	Status of holes	ACH@50Pa	ACH n_{CO2} (CO_2)	ACH n_{moist} (moisture)
A_1	all holes open (8x2 = 16cm^2)	1.1	0.074	0.040
A_2	all holes open (8x2 = 16cm^2)	1.1	0.088	0.024
A_3	all holes open (8x2 = 16cm^2)	1.1	0.049	0.068
A_4	only e_1-e_2-e_7-e_8 open (4x2 = 8cm^2)	0.5	0.040	0.023
A_5	only e_1-e_2-e_7-e_8 open (4x2 = 8cm^2)	0.5	0.043	0.034
A_6	only e_1-e_2-e_7-e_8 open (4x2 = 8cm^2)	0.5	0.055	0.030

In Fig. 5a the recordings from the sensors d_1-d_5 are shown. The results from the sensors d_3 and d_5 reveal that the CO_2 decay at the area of the ceiling is smoother than on the level of 55cm above the floor, i.e. d_2 and d_4, which are located closer to the leakages. The findings are consistent with previous studies, showing that the phenomena are more fluctuating at the neighbourhood of leakages (Kraniotis, 2014).

The logarithm of the normalized CO_2 concentration is shown against the time in Fig. 5b. The calculated infiltration rates based on the CO_2 decay, n_{CO2} are also depicted in Table 1. When all the 8 holes were open (A_1-A_3), n_{CO2} tends to be higher compared to the days that four of the holes were sealed (A_4-A_6). In addition, the tighter the room was, the smaller the variations among the infiltration rates.

In Table 1 the 'moisture-based' infiltration rates n_{moist} are also presented. The n_{moist} show smaller values compared to n_{CO2}. It would be reasonable to claim that n_{moist} can represent that in the cases A_4-A_6 the room was tighter, however the agreement between n_{CO2} and n_{moist} is rather not consistent. In contrast to the outdoors CO_2 levels, the vapour pressure and concentration outdoors are not constant (Fig.6). Thus, a 'vapours injection' from outdoors to indoors takes place even during the decay of indoors moisture making the calculation of 'moisture-based' infiltration rates more complex.

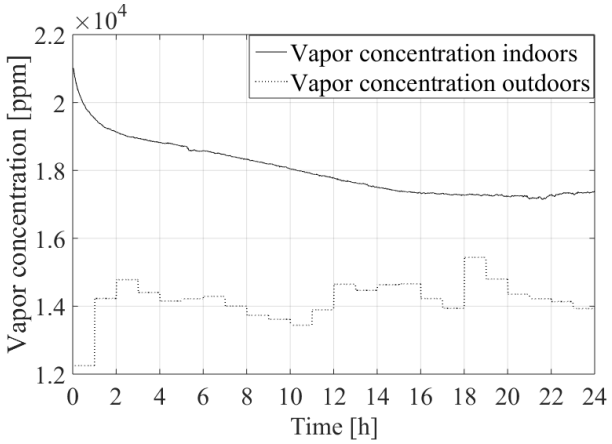

Figure 6: The vapour concentration indoors and outdoors during the phase 3 of test A_6.

In order to study the influence of local in- and exfiltration on moisture contents in the test house elements, the MC in some characteristic positions is shown (Fig. 7). The first two graphs show the results from the test A_3, in which all the 8 holes were open during the phase 3. All the four sensors presented are next to leakages and a similar behaviour is shown. However, the levels of MC is very low and it is rather ambitious to draw concrete conclusions based on the current findings.

The other two graphs of Fig. 7 present the some sensors from the test A_5. It is important to note that the tests A_3 and A_5 have similar infiltration rate calculated, i.e. 0.049 and 0.043 respectively, despite the fact that in A_3 8 holes were open while in A_5 only 4 of them. The

sensors next to open holes (leakages), i.e. S_6 and S_{11}, have similar behaviour as before. The comparison of S_6 and S_{11} though with the sensors S_8 and S_{13} that are located next to sealed holes during the test A_5, show small differences among the results. In particular, the sensors S_8 and S_{13} have a rather smoother decay compared to S_6 and S_{11}, revealing that the local infiltration phenomena is likely to have impact on the moisture drying process in hygroscopic surfaces. However, the fact that the room is quite tight results in narrowing down the influence. In addition, the low levels of MC makes more difficult to highlight the differences.

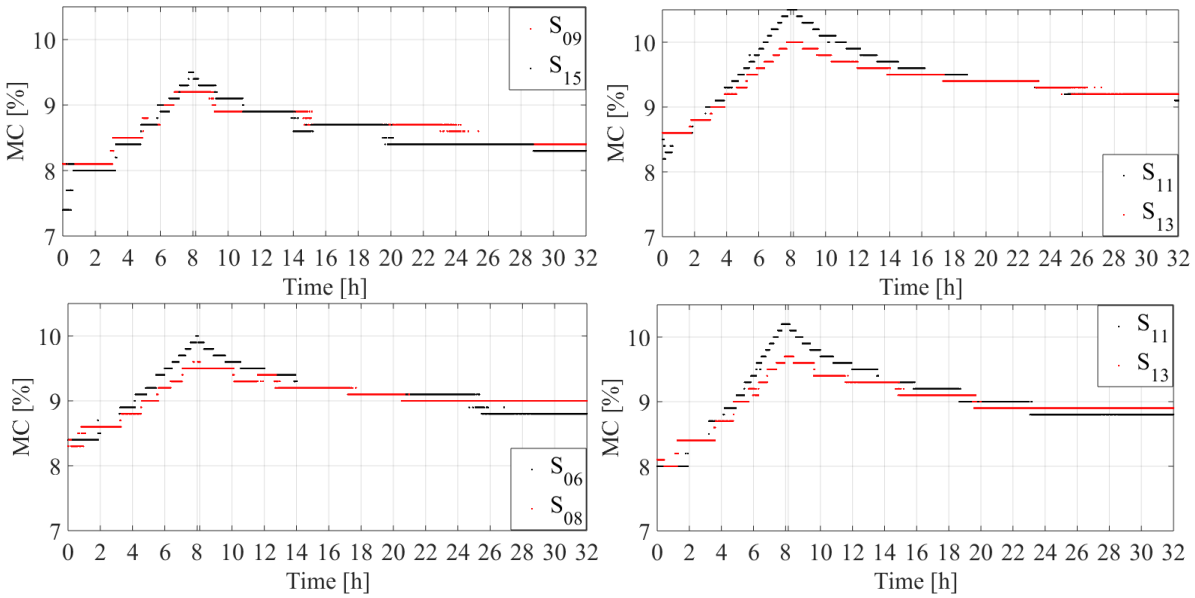

Figure 7: Moisture content MC in various positions (a) west wall and door in test A_3. (b) ceiling in test A_3. (c) north wall in test A_5. (d) ceiling in test A_5. (the detailed position of the sensors is shown in Fig. 3)

4 CONCLUSIONS

The current paper elaborates with simultaneous decay of CO_2 and vapours in a relatively tight and insulated cross laminated timber (CLT) test house, in order to investigate the influence of infiltration on moisture buffer (drying process). The results show that it is likely that the moisture content dries out faster in positions closer to leakages compared to the positions that are not close to them. Even when the global infiltration rates between two case-studies are very similar, differences on the moisture content can be observed based on where the leakages are located. However, the differences in the current set of experiments presented were rather small. The fact that the room is quite tight results in narrowing down the influence of in- and exfiltration on moisture buffer capacity. In addition, the low levels of MC makes more difficult to highlight these differences. The authors believe that the impact would be more clear in a looser building, where infiltration phenomena play significant role.

Moreover, the infiltration rates were calculated using both CO_2 and moisture (water vapours) as tracer gases. The result showed that using water vapours as tracer gas might be more complex because, in contrast to the outdoors CO_2 levels, the vapour pressure and concentration outdoors are not constant. Thus, a ‘vapours injection’ from outdoors to indoors takes place even during the decay of indoors moisture. Further elaboration with the latter could be of interest.

5 ACKNOWLEDGEMENTS

The authors want to thank the Norwegian Research Council (NRC) for funding this study in the context of the research project HOME – Holisitc Monitoring of Indoor Environment. The authors gratefully acknowledge Signe Kroken from NMBU for providing the meteorological data of Ås. Kolbjørn Mohn Jenssen, director of Mycoteam, is also acknowlegded for his valuable contribution to the execution of experiment.

6 REFERENCES

ASTM International E741-06. (2006). Standard test method for determining air change in a single zone by means of tracer gas dillution.

Haghighat, F., Brohus, H., Rao, J. (2000). Modelling air infiltration due to wind fluctuations – A review. *Building and Environment*, 35, 377-385.

Kraniotis, D., Aurlien, T. Thiis, T.K. (2014). Investigating instantaneous wind-driven infiltration rates using the CO_2 concentration decay method. *Int. Journal of Ventilation*, 13(2), 111-123.

Li, Y., Fazio, P., Rao, J. (2012). An investigation of moisture buffering performance of wood panelling at room level and its buffering effect on a test room. *Building and Environment*, 47, 205-216.

Osanyintola, O.F., Simonson, C.J. (2006). Moisture buffering capacity of hygroscopic building materials: Experimental facilities and energy impact. *Energy and Buildings*, 38, 1270-1282.

Rode, C., Peuhkuri, R., Mortensen, L.H., Hansen, K.K., Time, B., Gustavsen, A., Ojanen, T., Ahonen, J., Svennberg, K., Harderup, L.E,, Arfvidson, J. (2005), *Moisture buffering of building materials.* Project No.: 04023. Nordic Innovation Centre.

Rode, C., Grau, K. (2008). Moisture buffering and its consequence in whole building hygrothermal modeling. *Journal of Building Physics* 31, 333-360.

Roulet, C.A., Foradini, F. (2002). Simple and cheap air change rate measurement using CO_2 concentration decays. *Int. Journal of Ventilation*, 1 (1), 39-44.

Simonson, C.J., Salonvaara, M., Ojanen ,T. (2001). *Improving Indoor Climate and Comfort with Wooden Structures.* Technical Research Centre of Finland, VTT Publications 431. Espoo, Finland.

Simonson, C.J., Olutimayin, S., Salonvaara, M., Ojanen, T., O'Connor, J. (2004). *Potential for Hygroscopic Building Materials to Improve Indoor Comfort and Air Quality in the Canadian Climate.* ASHRAE Conference Proceedings 2004.

Yang, X., Fazio, P., Ge, H., Rao, J. (2012). Evaluation of moisture buffering capacity of interior surface materials and furniture in a full-scale experimental investigation, *Building and Environment*, 47, 188-196.

Yang, X., Ge, H., Fazio, P., Rao, J. (2014). Evaluation of parameters influencing the moisture buffering potential of hygroscopic materials with BSim Simulations. *Buildings, 4(3),* 375-393.

Yoshino, H., Mitamura, T., Hasegawa, K. (2009). Moisture buffering and effect of ventilation rate and volume rate of hygrothermal materials in a single room under steady state exterior conditions. *Building and Environment*, 44, 1418-1425.

Woloszyn, M., Kalamees, T., Abadie, M.O., Steeman, M., Kalagasidis, A.S. (2009). The effect of combining a relative-humidity-sensitive ventilation system with the moisture-buffering capacity of materials on indoor climate and energy efficiency of buildings. *Building and Environment*, 44, 515-524.